

Simultaneous observation of *in situ* water reflectance and atmospheric properties from autonomous sensor systems to improve satellite validation of optically complex waters

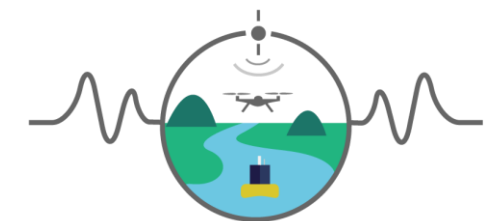
Tom Jordan¹, Stefan Simis¹, Philipp Grötsch²

John Wood³, Nick Selmes¹

1. Plymouth Marine Laboratory, UK. 2. Gybe, USA. 3. Peak Design, UK.



This project has received funding from the European Union's Horizon 2020 research and innovation programme under grant agreement No 776480



MONOCLE

Multiscale Observation Networks for Optical
monitoring of Coastal waters, Lakes and Estuaries

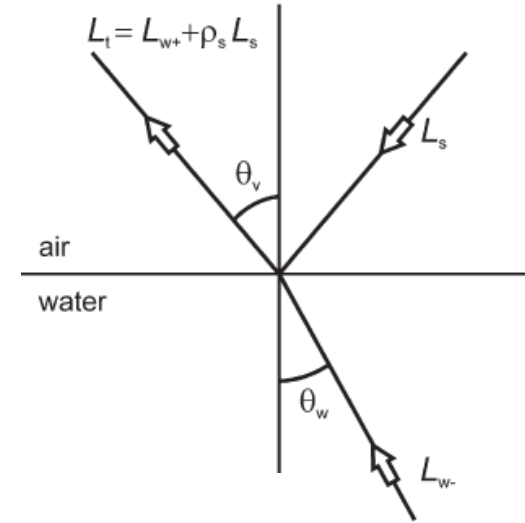
Talk overview

- 1. Autonomous sensor systems and deployments in MONOCLE**
 - So-Rad (Solar tracking Radiometry platform): $L_s, L_t, E_d \rightarrow R_{rs}$
 - HSP (Hyperspectral Pyranometer): $E_d, E_{ds}, E_{dd} \rightarrow AOT$
- 2. A new way to retrieve *in situ* R_{rs} by combining So-Rad and HSP**
 - Modification of R_{rs} algorithm (3C) to incorporate direct-diffuse irradiance from the HSP.
 - Illustration of improved precision in R_{rs} .
- 3. Spatial scales of R_{rs} variability from 'ships of opportunity'**
 - Measuring sub-pixel variability and spatial autocorrelation in R_{rs} .
 - Advantage to using mobile platforms for satellite validation.

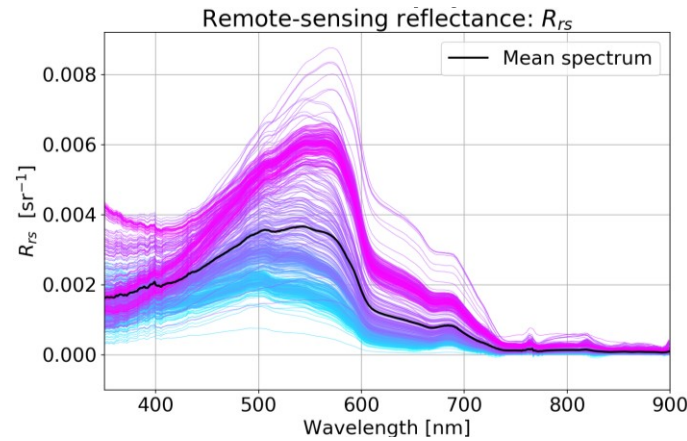


1.1 So-Rad (Solar-tracking Radiometry Platform)

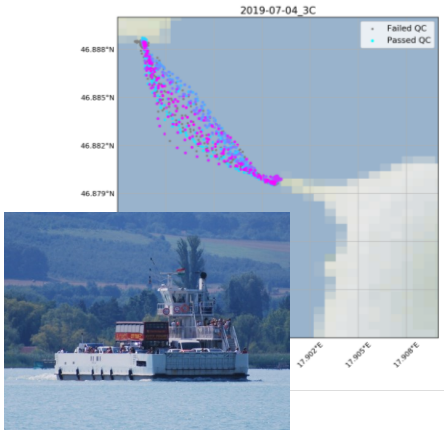
- Rotating platform designed to operate spectroradiometers on moving vessels whilst avoiding sun glint. Prototype in Simis and Olsson 2013.
- Applications of Rrs: ecosystem monitoring and satellite validation (assessment of atmospheric correction uncertainty & sub-pixel variability).
- Stand-alone operation (except cleaning), low power consumption (15 W), low cost (~€ 3000 + sensors). Open-source compatible with Linux on a Raspberry Pi 3B.



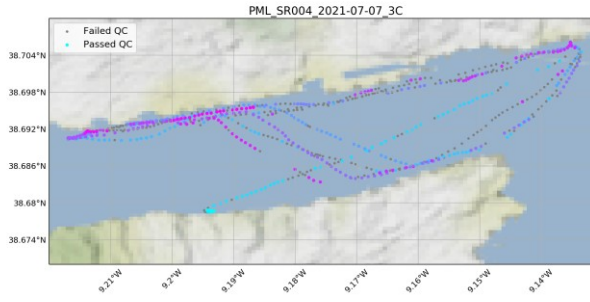
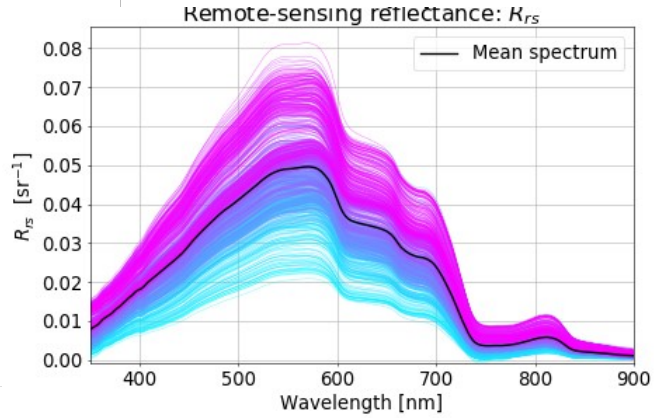
$$R_{rs}(\lambda) = \frac{L_t(\lambda)}{E_d(\lambda)} - \rho \cdot \frac{L_s(\lambda)}{E_d(\lambda)}$$



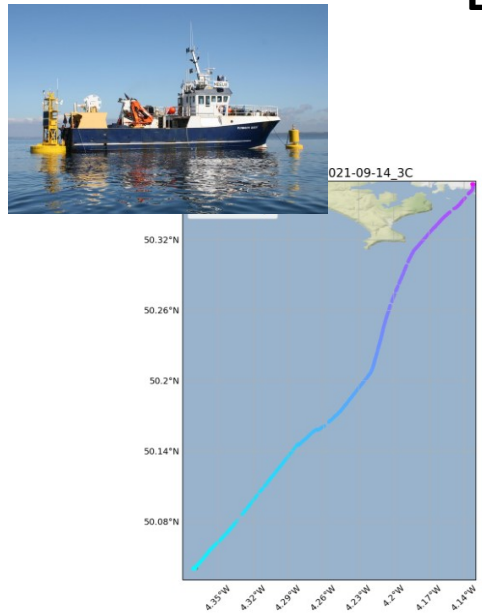
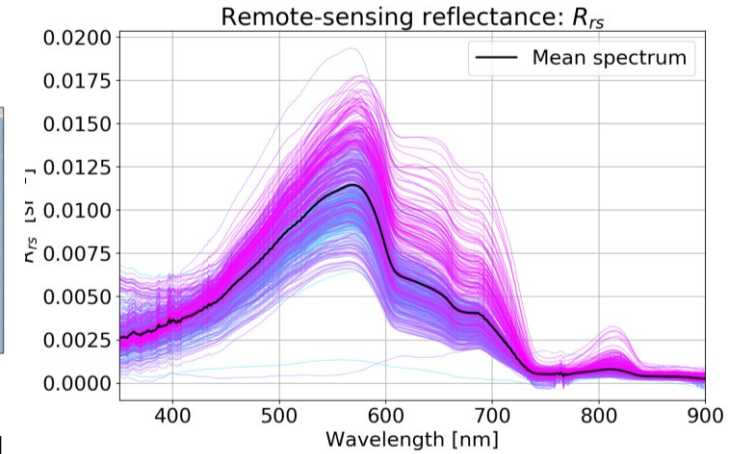
1.2 Spatial variability in R_{rs} from So-Rad on 'ships of opportunity'



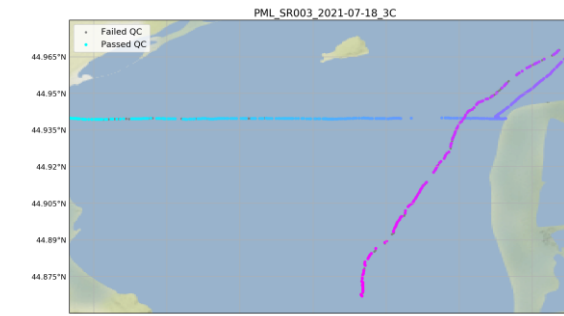
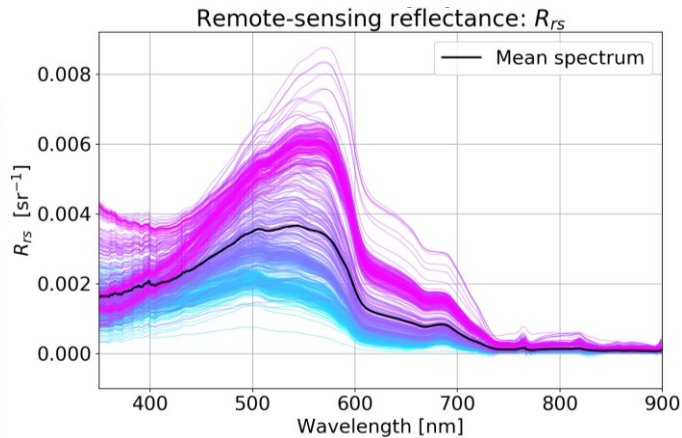
Lake Balaton, Hungary



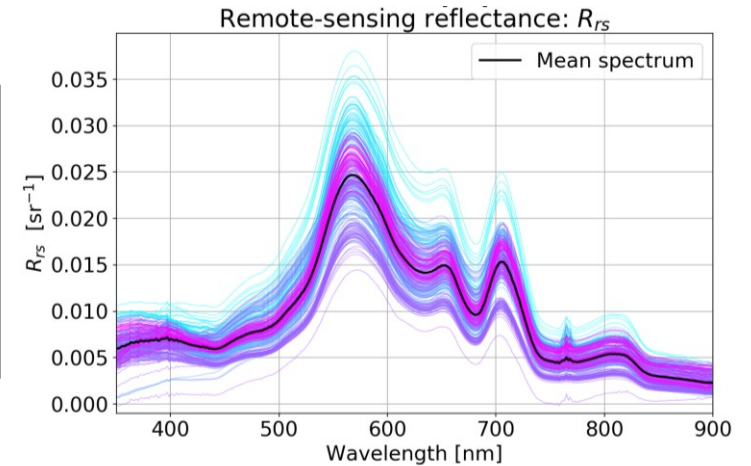
Tagus Estuary, Portugal



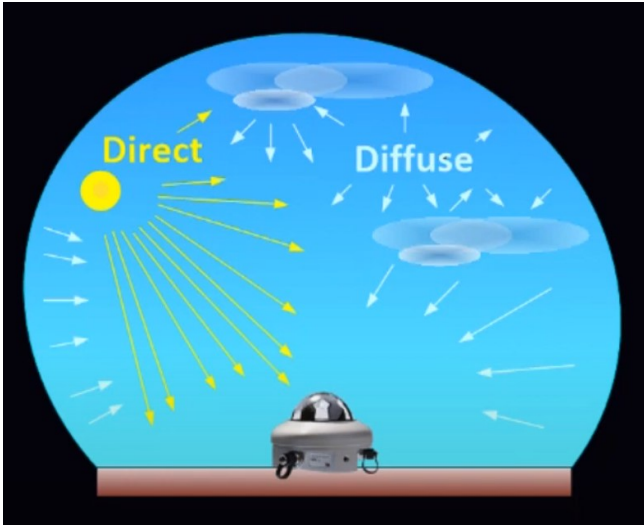
Plymouth Sound and near-coast, UK



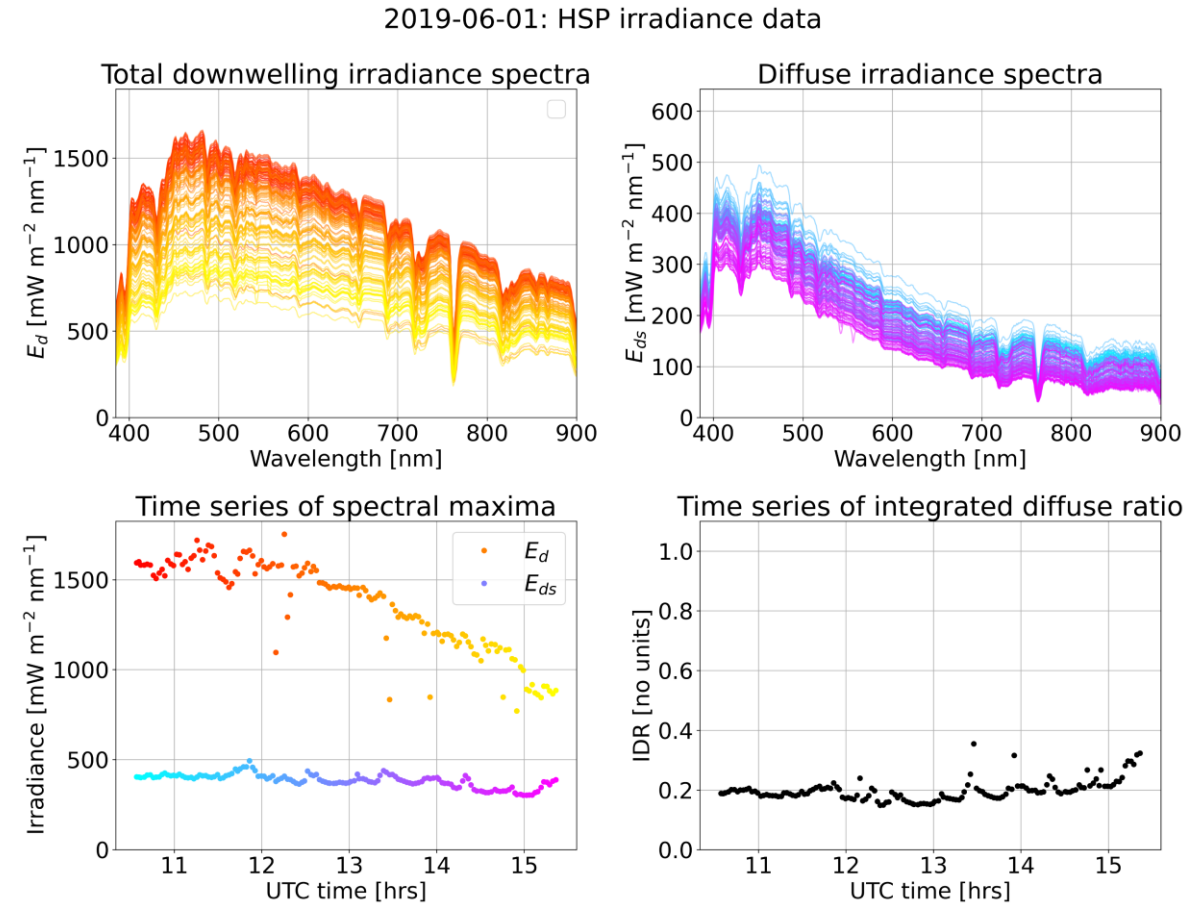
Danube Delta, Romania



1.3 Direct-diffuse irradiance from the Hyperspectral Pyranometer (HSP)



- Partitions E_d (downwelling irradiance) into direct (E_{dd}) and diffuse (E_{ds}) components.
- Primary usage: characterization of aerosol optical thickness (AOT).
- Incorporates a shading pattern over multiple diffuser optics: can be operated on moving platforms. Prototype in Wood et al. 2017.



2.1 The 3C (3 glint component) Rrs algorithm

- **3C algorithm** (Groetsch et al. 2017): Rrs derived from spectral optimization using water (Albert & Mobley, 2003) and atmospheric (Gregg & Carder, 1990) models.
- **Spectral-offset, $\Delta(\lambda)$** : ‘additional spectral’ basis functions (E_{dd}/E_d , E_{ds}/E_d).
- **Rationale**: improved estimation of Rrs when L_s/E_d is not representative of surface-reflected radiance (wind-roughened & scattered-cloud conditions).
- **Current limitation**: spectral shape of E_{dd}/E_d and E_{ds}/E_d based on model inversion (uses clear-sky model).

Conventional above-water Rrs equation:

$$R_{rs}(\lambda) \equiv \frac{L_w(\lambda)}{E_d(\lambda)} = \frac{L_t(\lambda)}{E_d(\lambda)} - \rho_s \frac{L_s(\lambda)}{E_d(\lambda)} - \delta$$

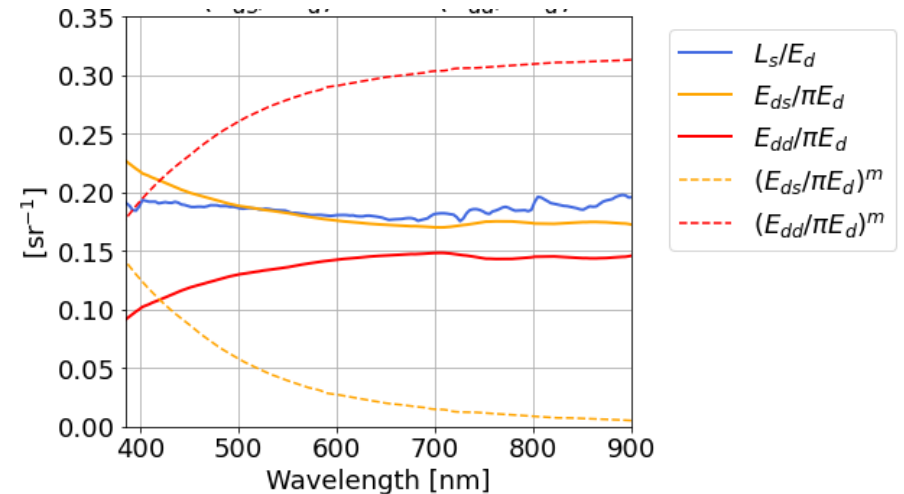
Rrs equation in 3C:

$$R_{rs}(\lambda) \equiv \frac{L_w(\lambda)}{E_d(\lambda)} = \frac{L_t(\lambda)}{E_d(\lambda)} - \rho_s \frac{L_s(\lambda)}{E_d(\lambda)} - \Delta(\lambda),$$

$$\Delta(\lambda) = \frac{\rho_{dd}}{\pi} \cdot \left(\frac{E_{dd}(\lambda)}{E_d(\lambda)} \right)^m + \frac{\rho_{ds}}{\pi} \cdot \left(\frac{E_{ds}(\lambda)}{E_d(\lambda)} \right)^m,$$

Example of ‘glint basis functions’:

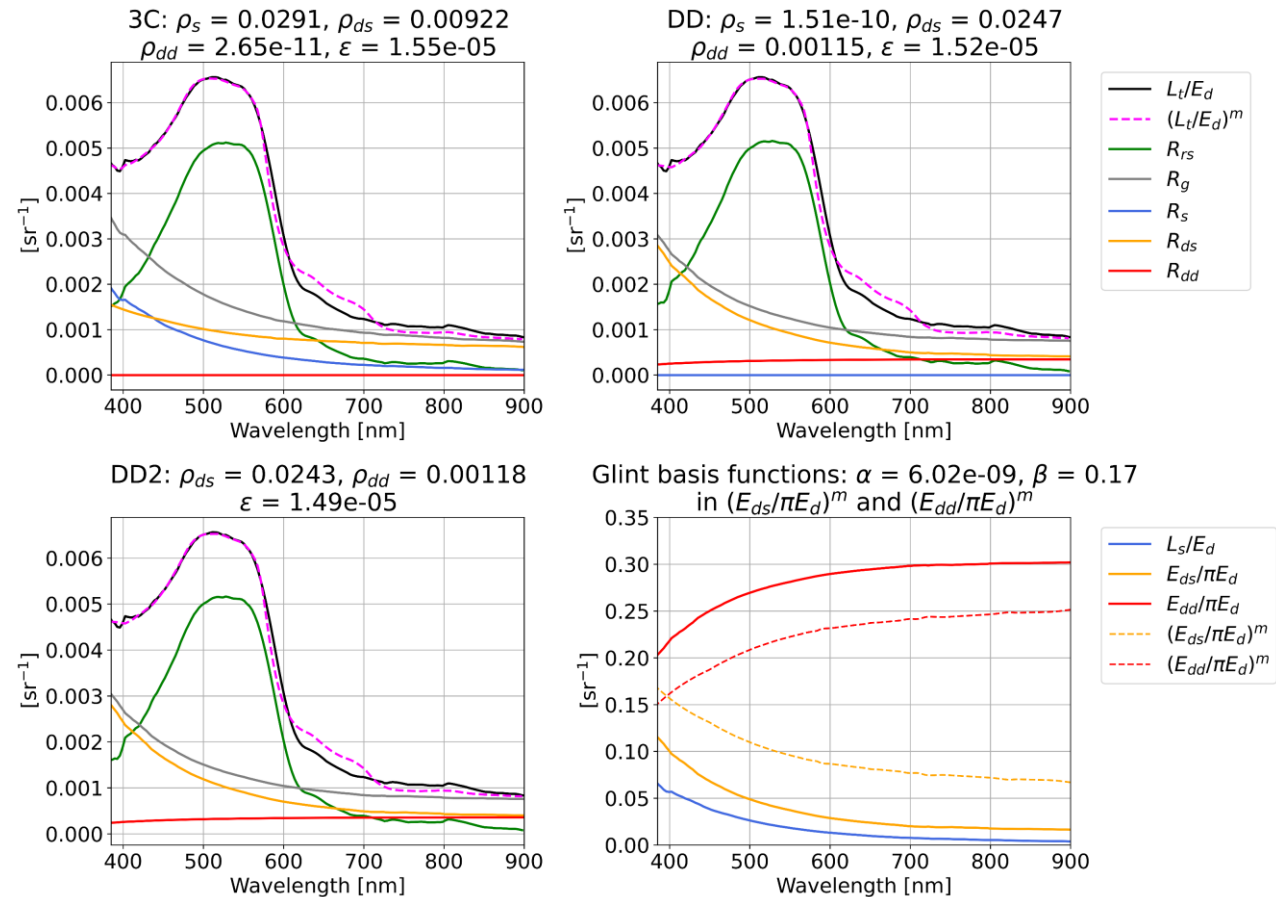
Dashed lines: model-optimized by 3C
 Solid lines: measured by HSP



2.2 A new way to retrieve *in-situ* Rrs by combining So-Rad and HSP

- **Central idea:** HSP measurements of E_{ds}/E_d and E_{dd}/E_d replaced model-optimized glint terms in 3C.
- **Hypothesis:** HSP measurements will better-constrain the spectral-shape of glint correction (& remove atmospheric-model dependence).
- We benchmarked 3 algorithm variants:
 1. **3C** (3 component glint): model optimization for E_{ds}/E_d and E_{dd}/E_d
 2. **DD** (direct-diffuse): HSP measurements for E_{ds}/E_d and E_{dd}/E_d .
 3. **DD2:** 2-sensor variant of DD (no L_s sensor & lower cost solution).

2020-07-30 09:00:38, IDR: 0.0646



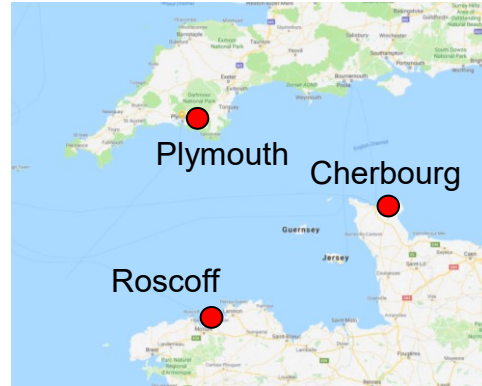
Incorporating a hyperspectral direct-diffuse pyranometer in an above-water reflectance algorithm.

Jordan et al. 2022, *Remote Sensing*, 14, 2491.

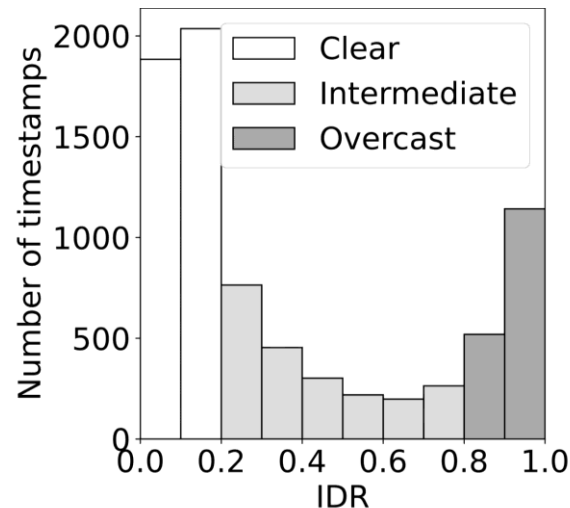
2.3 Deployment & atmospheric characterization using the HSP

- ~ 4.5-month time series of in-port data from the Western Channel (summer 2020).
- So-Rad and HSP deployed on *Armorqiu* (Brittany Ferries) & collecting (near)-simultaneous data.
- Atmospheric state variable: Integrated Diffuse Ratio ('fraction of diffuse light')

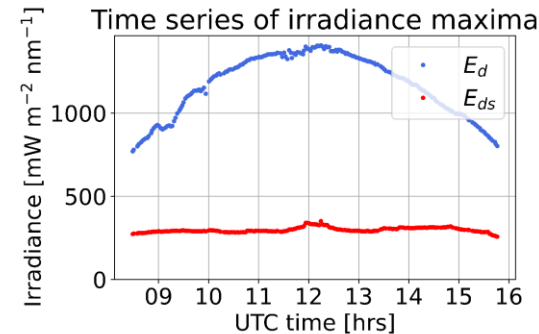
$$IDR = \frac{\int_{\lambda_i}^{\lambda_f} E_{ds}(\lambda) d\lambda}{\int_{\lambda_i}^{\lambda_f} E_d(\lambda) d\lambda}$$



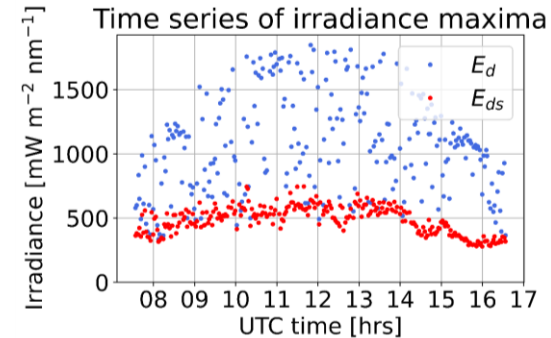
Distribution of IDR for deployment



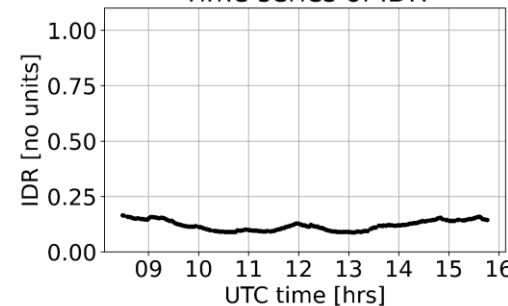
2020-04-15: Clear conditions



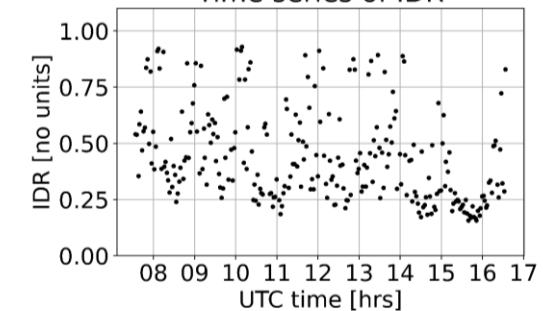
2020-05-23: Intermediate conditions



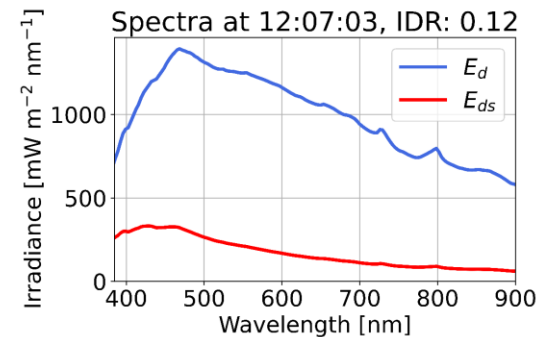
Time series of IDR



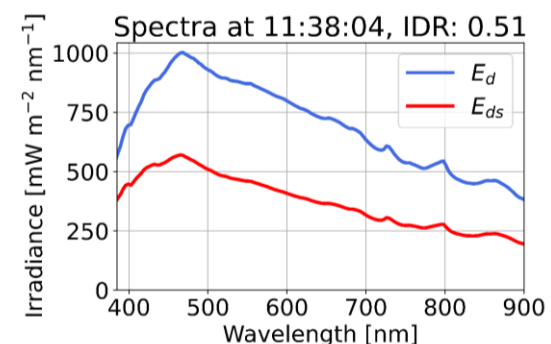
Time series of IDR



Spectra at 12:07:03, IDR: 0.12

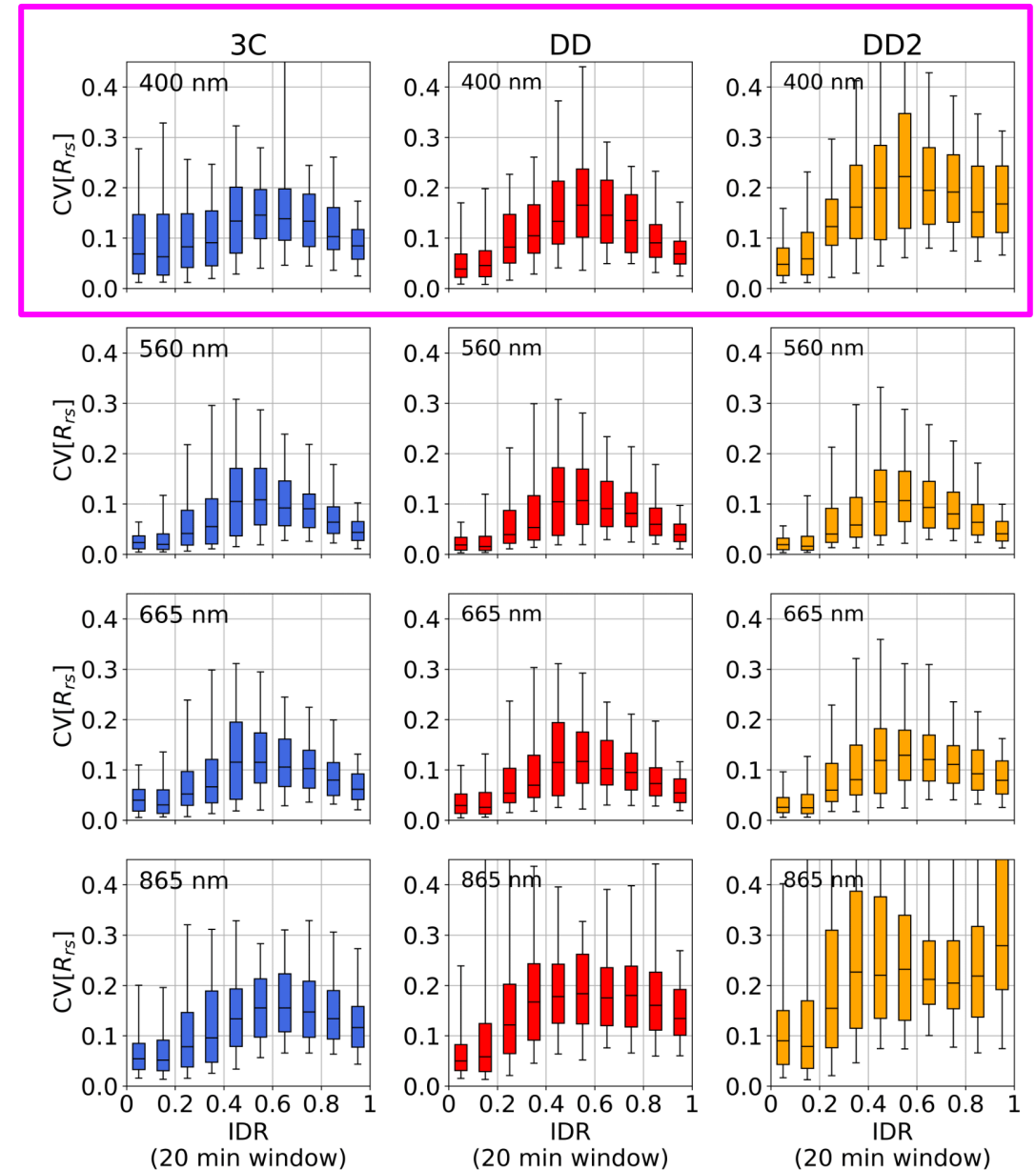


Spectra at 11:38:04, IDR: 0.51



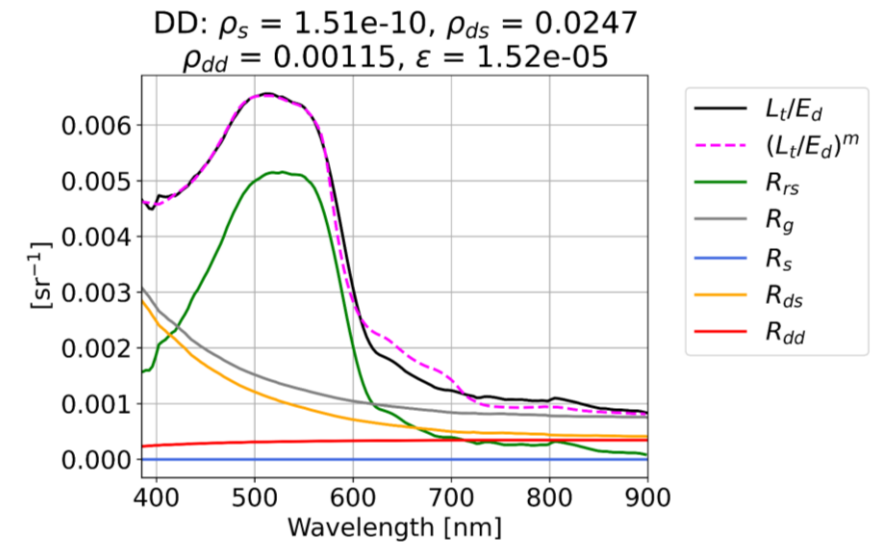
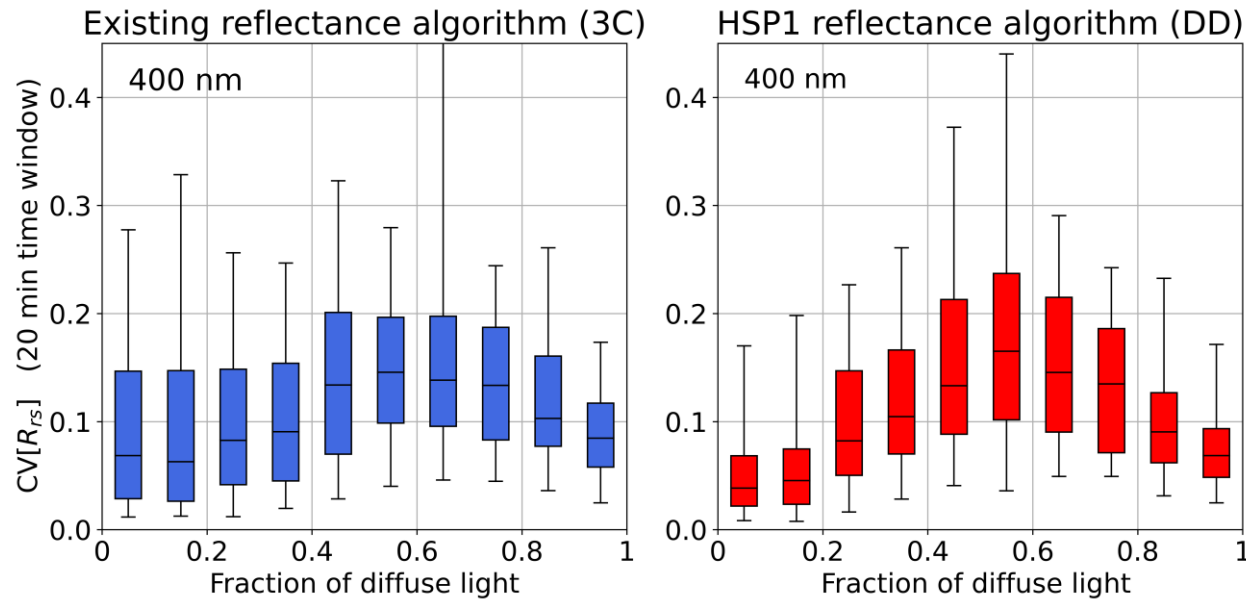
2.4 Dependence of algorithm precision on atmospheric conditions

- Assess algorithm precision over 20-minute measurement cycles using R_{rs} coefficient of variation.
- **Key result:** DD has significantly lower variability than 3C in clear conditions ($IDR < 0.2$) in the blue (400 nm) band.
- DD and 3C have comparable variability in green (560 nm), red (665 nm), and NIR bands (865 nm).
- All algorithms have relatively high variability in intermediate conditions (scattered cloud). DD2 has higher variability than 3C and DD in overcast conditions.



2.5 Improved Rrs precision at blue wavelengths using the HSP

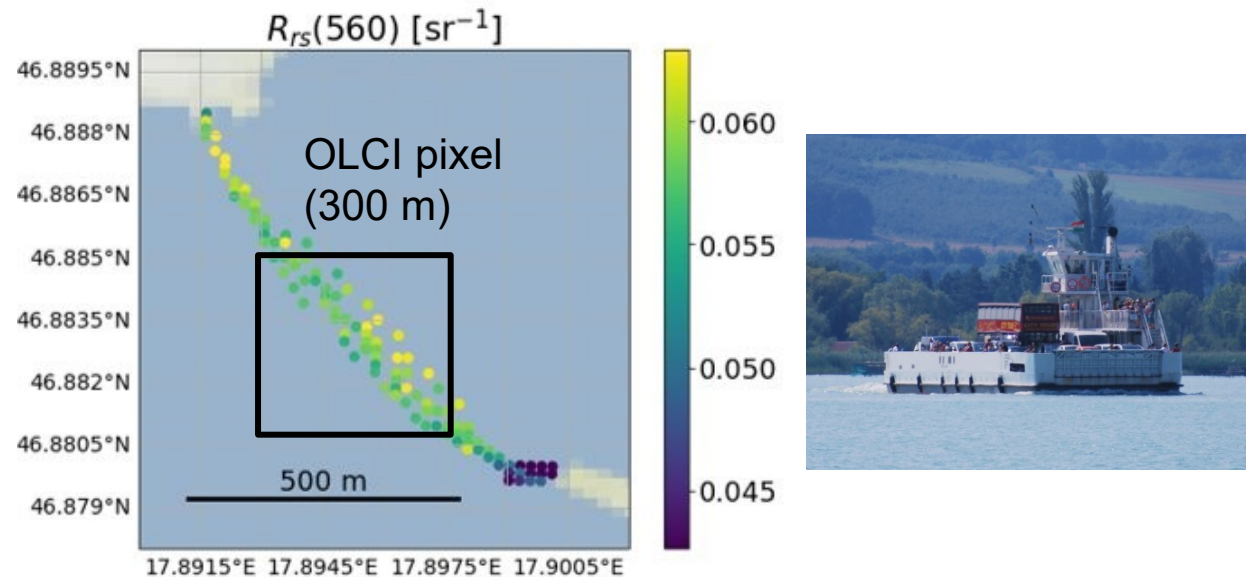
Improved precision of DD at blue wavelengths: consistent with the spectral curvature of the glint correction being better constrained (via HSP measurements).



3.1 Using ‘ships of opportunity’ to sample sub-pixel variability for satellite validation

- Satellite validation: assessment of ‘match-ups’ between *in-situ* Rrs (~ point-like data) and satellite Rrs (information aggregated over pixel: 300 m for OLCI, 10-60 m for MSI).
- ‘Mismatch in spatial scales’ can contribute to uncertainty budget in match—up analysis (particularly if a fixed-platform is used to measure Rrs).
- Here we illustrate the advantage to using a mobile platform to sample sub-pixel variability: Lake Balaton car ferry deployment used as case study.

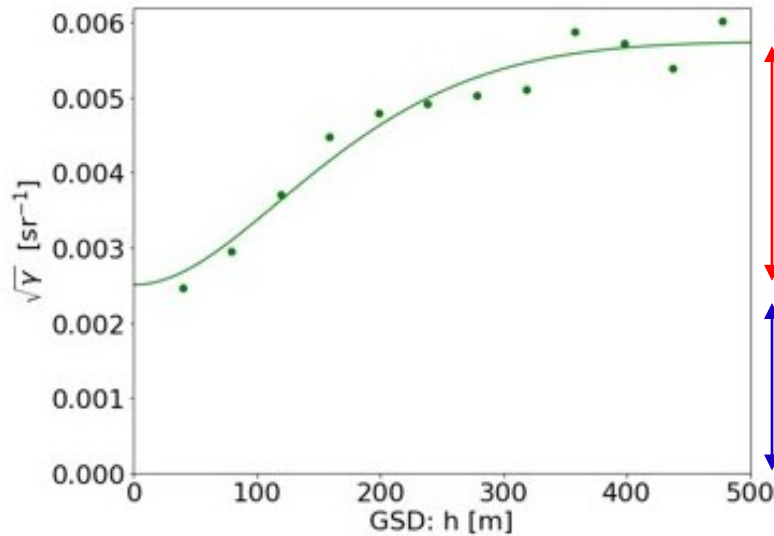
Rrs(560) collected by So-Rad within a 6hr match-up window from Lake Balaton car ferry



3.2 Characterizing spatial scales of *in situ* Rrs variability

- Variogram methods were used to sample spatial variation in Rrs as a function of mean ground sample distance (GSD: h).

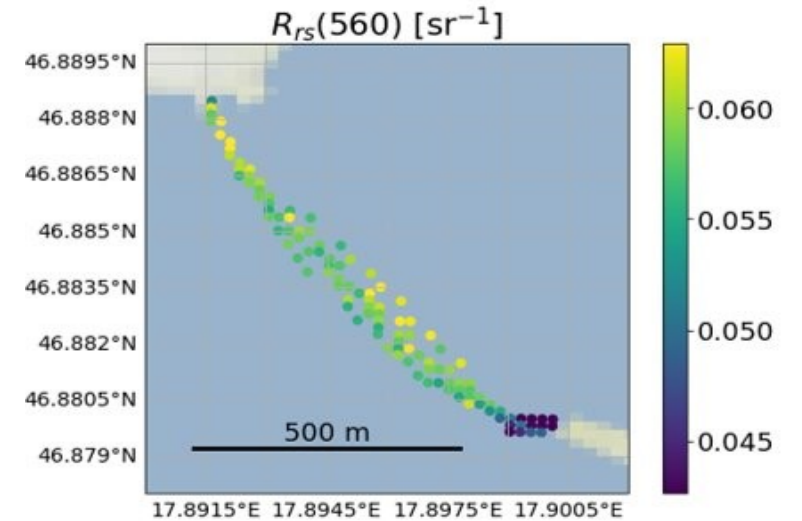
‘Root variogram’: dependence of STD Rrs on point separation



Spatial variation in Rrs

Intrinsic variation in Rrs: includes instrument noise, algorithm uncertainty, temporal variation within match-up window.

Correlation length (distance over which Rrs is spatially autocorrelated)



Fitted (Gaussian) model

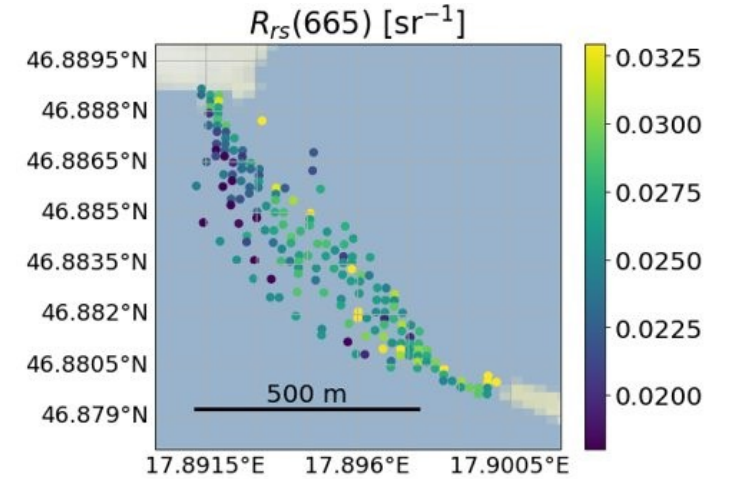
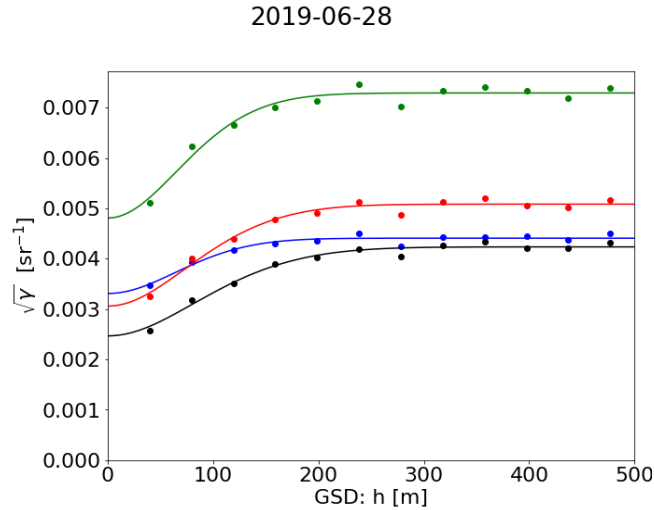
Empirical semi variance:
$$\gamma(h) = \frac{1}{2N(h)} \sum_{i \neq j} [R_{rs}(x_i) - R_{rs}(x_j)]^2$$

$$\gamma(h) = C_0 + (C_\infty - C_0)(1 - \exp(-4h^2/L^2))$$

3.3 Examples of root-variograms from the Lake Balaton deployment

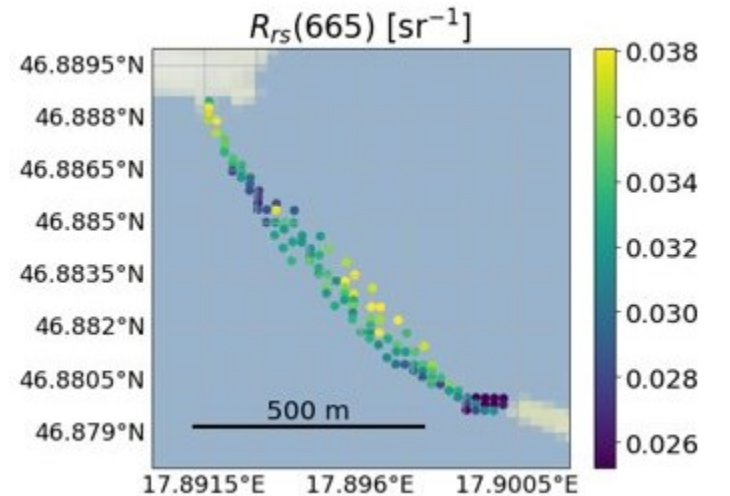
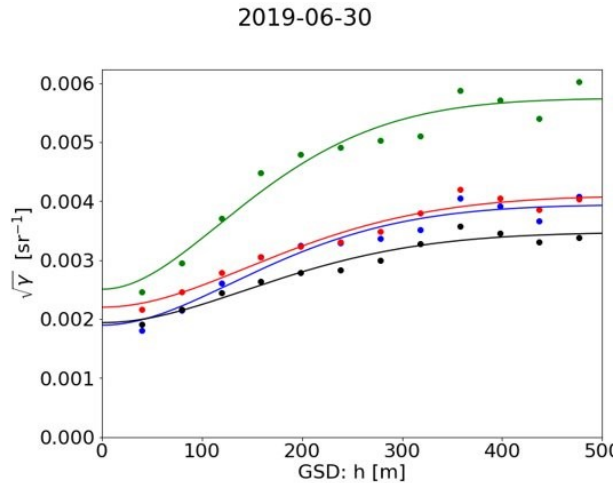
Case of lower structural variation in Rrs: shorter correlation length, and lower ratio of spatial-intrinsic variance: 'Patchier water'

443 nm : fit error = 2.4%, L = 1.97e+02
$\sqrt{C_0} = 0.00331, \sqrt{C_\infty} = 0.00441$
560 nm : fit error = 3.38%, L = 2.08e+02
$\sqrt{C_0} = 0.00481, \sqrt{C_\infty} = 0.00729$
665 nm : fit error = 3.05%, L = 2.42e+02
$\sqrt{C_0} = 0.00306, \sqrt{C_\infty} = 0.00508$
705 nm : fit error = 2.87%, L = 2.72e+02
$\sqrt{C_0} = 0.00247, \sqrt{C_\infty} = 0.00423$



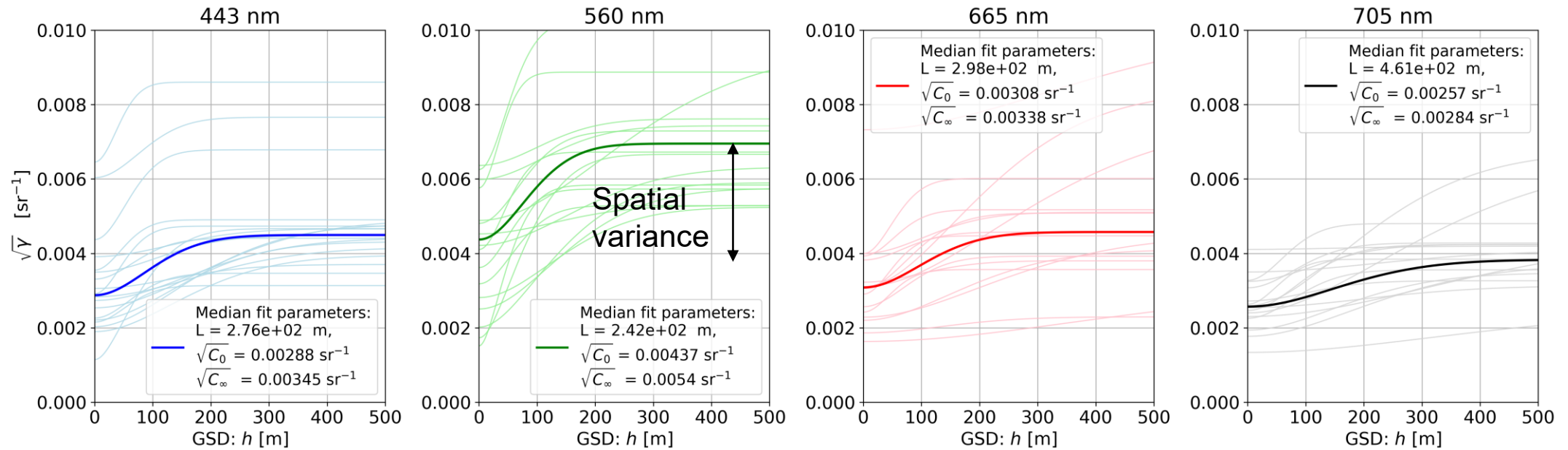
Case of higher structural variation in Rrs: longer correlation-length, and higher ratio of spatial-intrinsic variance

443 nm : fit error = 9.25%, L = 4.64e+02
$\sqrt{C_0} = 0.0019, \sqrt{C_\infty} = 0.00394$
560 nm : fit error = 8.81%, L = 4.36e+02
$\sqrt{C_0} = 0.00251, \sqrt{C_\infty} = 0.00575$
665 nm : fit error = 5.98%, L = 5.01e+02
$\sqrt{C_0} = 0.0022, \sqrt{C_\infty} = 0.0041$
705 nm : fit error = 6.1%, L = 4.87e+02
$\sqrt{C_0} = 0.00194, \sqrt{C_\infty} = 0.00347$



Data from 'hypothetical match-up windows' of 6 hrs.

3.4 Summary of root-variogram structure for the Lake Balaton deployment



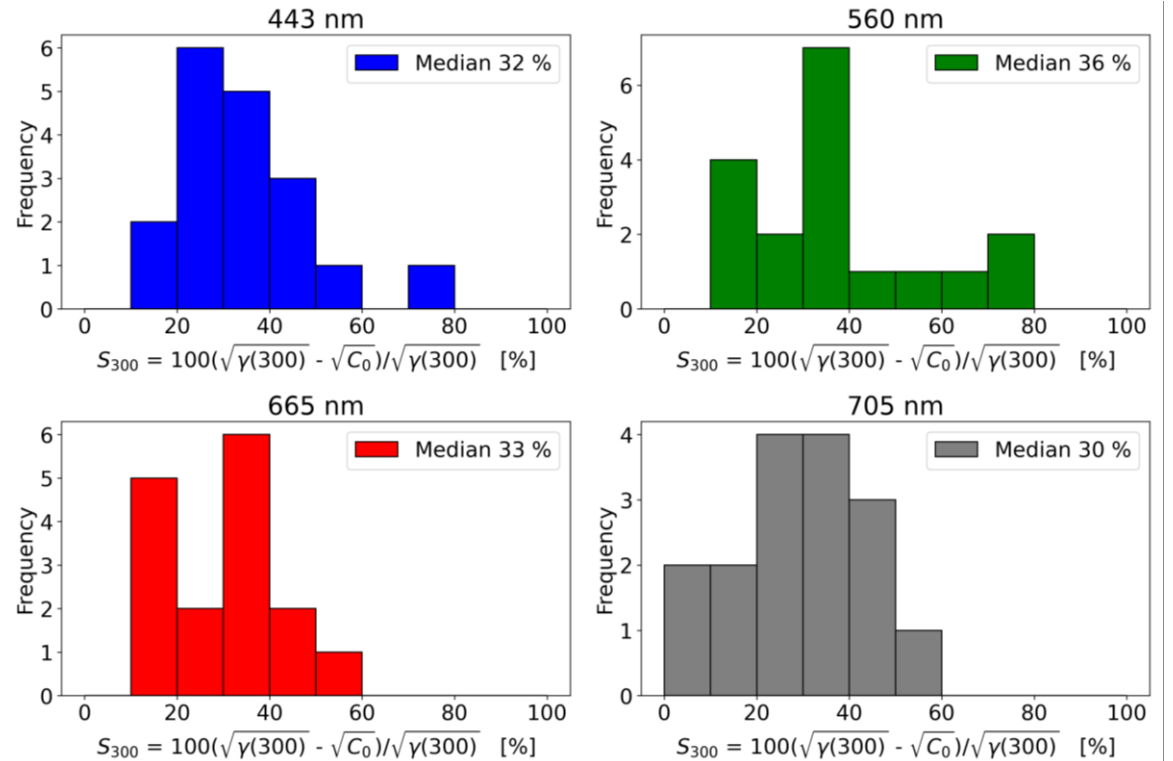
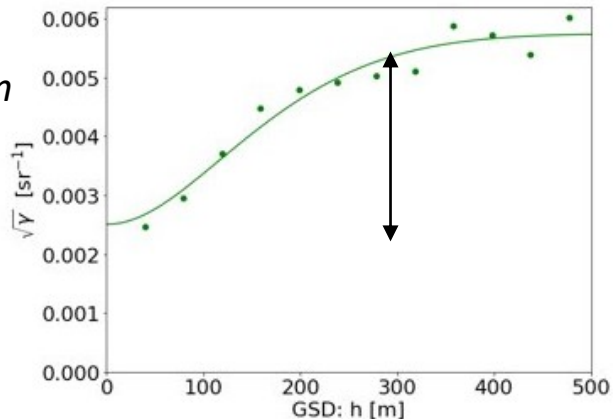
- Gaussian model fits are shown (subject to fit-filtering) . **Median fits in bold.** Corresponds to ~ 20 (hypothetical) match-up windows from a 6-week deployment on the car ferry
- Broadly similar shape of variogram between spectral bands
- Correlation lengths for Rrs ~ 100-400 m. Spatial variance component ~ 20-50% of total variance.

3.5 Percentage of Rrs variation due to spatial structure at 300 m (OLCI pixel size)

- Approximates additional % uncertainty that a fixed platform would experience in match-up analysis (due to not sampling sub-pixel variability).
- Alternatively, approximates % reduction in uncertainty that sampling Rrs from a moving platform enables (for large N).

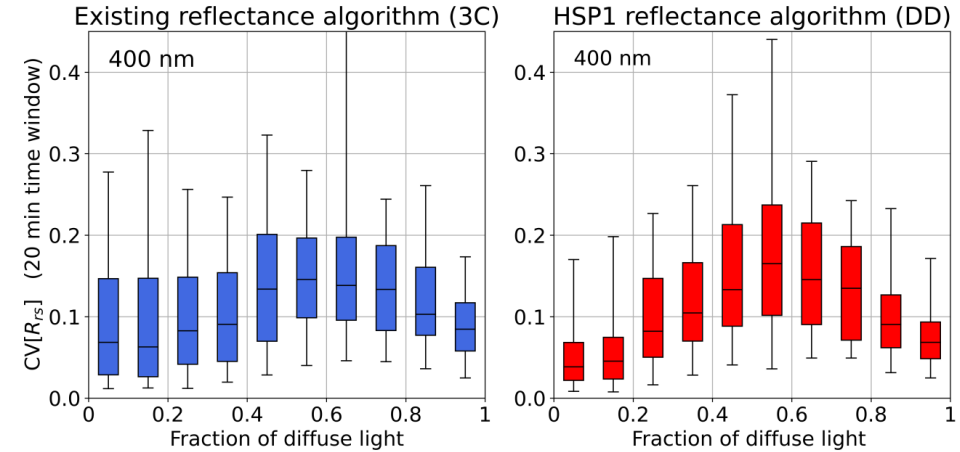
Variability in Rrs due to spatial structure at 300 m

(strictly: integrate variogram curve over point-separation distribution for pixel for better estimate)

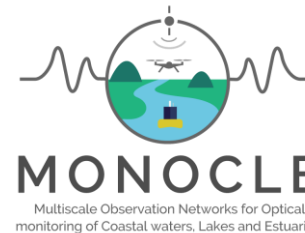
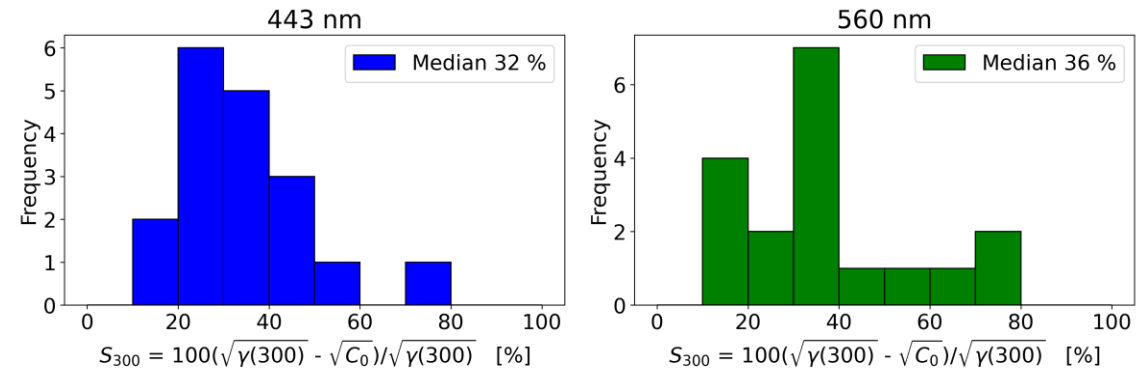


Summary and highlights

1. HSP and So-Rad are autonomous sensor systems, suitable for moving platforms that can aid satellite validation of R_{rs} in inland and coastal waters.
2. Combining So-Rad and the HSP in R_{rs} processing can improve the precision of *in-situ* R_{rs} (relative to baseline of 3C).
3. Sampling sub-pixel R_{rs} variability from a 'ship of opportunity' would reduce *in-situ* uncertainty by factor $\sim 1/3$ in OLCI match-up analysis (relative to sampling at a fixed location where water properties are unchanging).



Percentage of R_{rs} variability (STD metric) due to spatial structure at 300 m (OLCI pixel size)



<https://monocle-h2020.eu/>

tjor@pml.ac.uk